20th International Congress on Sound & Vibration

ICSV20
Bangkok,Thailand
7-11 July 2013

MRI SCANNER VIBRATION PATH ANALYSIS

Khan Imran, Gertsovich Irina, Claesson Ingvar and Håkansson Lars

Department of Electrical Engineering, Blekinge Institute of Technology, 371 79 Karlskrona, Sweden. e-mail:imran.khan@bth.se

Johansson Per-Erik, Wirenstedt Maria and V. Borja Oscar

Blekinge County Hospital, 371 85 Karslkrona, Sweden.

Petersson. J Stefan

MR Division, GE Healthcare, Stockholm, Sweden.

Magnetic Resonance Imaging (MRI) scanner is one of the most important tools in clinical diagnostics. MRI scanners are associated by strong vibration which results in unpleasant and disturbing acoustic noise. The primary source of this vibration is the Lorentz force produced by fast switching of the currents inside the gradient coils of MRI scanners under a strong static magnetic field. During an MR-imaging scan the switching is controlled in order to spatially code the hydrogen nuclei that will generate the signal, which is reconstructed into anatomical images. Faster switching of the currents allows for shorter scan times and/or higher image resolutions. Consequently, the clinical quality has motivated the drive for shorter switching time and higher currents. This development, however, has also caused an undesired increase of MRI vibrations. The overall vibration phenomenon of an installed fully functional MRI scanner system becomes unique because of the installed location and ambiance. This vibration can potentially degrade the image quality and hence the diagnosis. Apart from the vibration produced, the associated annoying acoustic noise may not only affect the patients under examination and the clinical staff, but may also be transmitted to other parts of the building and causing discomfort for the personnel working there. In order to devise an effective isolation plan or improve an existing one both for vibration and acoustic noise it is important to study the noise and vibration transfer paths. This paper concerns an investigation of vibration transfer paths for vibration excited by an installed functional MRI scanner at a medical facility. The vibration transfer paths have been investigated experimentally. The obtained results are presented and discussed.

1. Introduction

The clinical diagnostic quality of Magnetic Resonance Imaging (MRI) scanner has improved at the cost of increased vibration level during operation in recent years. The main reason is that faster scanning techniques and higher currents are employed in new MRI scanners resulting in higher Lorentz forces. Consequently, the increased vibration and associated unpleasant acoustic disturbance also demand careful structural design of the installation site and more effective silencing techniques[1].

Most of the efforts are aimed to design quite MRI scanners by isolating the gradient coils[2,3,4,5]. However, the vibration problem still remains at large. Every installed location and surrounding ambiance of a functional MRI scanner present unique challenges concerning vibration isolation and silencing measures. The vibration can be transmitted to other parts of the location and not only cause structural damage but can also affect operation of other sensitive equipment in the proximity. The acoustic disturbance may transmit to the surrounding areas both through air, known as air born noise or through the floor or walls etc. termed as structure born noise. The vibration isolation becomes even more challenging when a new MRI scanner is installed at an existing facility. Apart from the vibration isolation, some structural reinforcement may also be required. In order to devise a successful isolation plan or improve an existing one both for vibration and acoustic noise it is important to quantify or study the noise and vibration transfer paths. A study of such vibration paths of a functional MRI scanner installed at Blekinge County hospital Karlskrona, Sweden, is the subject of this paper. The vibration transfer paths are measured experimentally with the help of the trasnmissibilty function concept.

2. Vibration transfer path analysis

Transfer path analysis (TPA) is an important tool to identify operational forces and vibration transfer paths in order to study the Noise Vibration and Harshness (NVH) behaviour of a system. Several experimental methods exist to determine the vibro-acoustic paths. In the classical TPA the system's frequency response function (FRF) is measured by exciting the system with an impulse hammer or shaker and measuring the response. Synthesized responses are then generated by combining the FRF and operational forces, from which the contribution by each noise path is determined. The TPA can be performed either by disassembling the system or taking the whole system without disassembling[6]. The former method avoids the coupling problems but is time consuming and most importantly the boundary conditions are changed. The later technique eliminates these drawbacks. Another technique known as operational transfer path analysis (OTPA) determines the transsmisibilty matrix i.e response to response transfer function for determining the vibration transfer paths using operational data[7]. This technique is similar to multi input multi output (MIMO) methods for determining the FRF. The transmissiblity frequency function or simply transmissibilty is the ratio between an output (response) and a reference response without the knowledge of the excitation forces. The responses can be any quantity of motion i.e. displacement, velocity or acceleration. The transmissibility concept applied to transfer path analysis stems from the fact that the equation of motion for a multi degree of freedom (MDOF) system may in the frequency domain be expressed as[8],

$$[H(f)]\{F(f)\} = \{X(f)\} \tag{1}$$

Where $[H(f)]$ is known as the FRF matrix, $\{X(f)\} = [X_1(f)X_2(f)\cdots X_M(f)]^T$ is the response vector in frequency domain and $\{F(f)\} = [F_1(f)F_2(f)\cdots F_M(f)]^T$ is the excitation force vector in frequency domain. The transmissibility or the ratio between two responses of different degrees-of-freedom $T_{ji}(f)$ is defined as

$$T_{ji}(f) = \frac{X_j(f)}{X_i(f)} \tag{2}$$

Equations (1) and (2) assumes that the Fourier Transform is defined for the responses and forces. However, in practice the transmissiblity is calculated using the H_1 estimator i.e. from the ratio of the cross spectrum $G_{X_jX_i}$ and the auto spectrum $G_{X_iX_i}$ of the two responses[9,10]. It is important to note that the transmissibility is different from the FRF i.e. the poles of $T_{ji}(f)$ are different from that of $[H(f)]$, therefore, the peaks in the transmissibility do not correspond to the resonance frequencies of the system[10]. The transmissibility concept has been successfully used to identify mode shapes and operational deflection shapes ODS[8,10,11]. In this paper we use the transmissibility function to study the vibration transfer paths.

3. Experimental setup

The measurements were conducted on the MRI scanner. The floor in the MRI room supports the MRI scanner's four feet via a vibration isolator at each foot.

3.1 Top view of the MRI scanner room

To understand the measurements procedure an approximate MRI scanner installation site is shown in Fig. 1, as seen from the top, without any proper scale. The MRI feet are numbered from 1 to 4. The sliding bed for the patients is omitted from the drawing as its weight and hence the vibration transfer is negligible as compared to the MRI. The encircled crosses show the floor positions where the acceleration signal is to be measured on the floor adjacent to each foot.

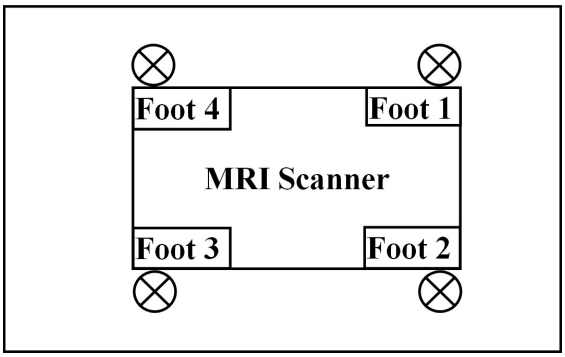

Figure 1. Top view sketch of the MRI room with MRI scanner.

3.2 Measurement equipment and procedure

As mentioned in the beginning of the current section the MRI scanner rest on the floor through its four feet via vibration isolation. The operational forces are unknown and due to the strong (3 Tesla) magnetic field an impulse hammer with force transducer may not be used for impulse excitation to measure FRF. However, it is possible to measure acceleration both on the feet of the MRI and floor positions beside each foot. Therefore, the transmissibility function is well suited to study the vibration transfer paths in this case. Accelerometers were glued to the MRI scanner feet with non magnetic (Brass) studs, to measure acceleration in the vertical direction. An accelerometer was glued to the floor adjacent to each foot position. The transmissibility between the responses i.e. acceleration spectra on a foot and adjacent floor position, denoted by i and j respectively is represented as $T_{ji}(f)$

The MRI scanner environment is characterized by a strong 3 Tesla magnetic field. Therefore, it is important that the measurement equipment e.g. accelerometers and the impulse hammer etc. used are not ferromagnetic. It is equally important that the performance of the sensors and measurement equipment should not be degraded by the presence of strong magnetic field. The equipment used in the measurements are chosen to be suitable for the MRI environment and are listed in Table. 1. The measured data is analysed in Matlab.

Table 1. Equipment used for MRI measurement.

Name	Tech Part. No	Quantity	Material
Accelerometer 3.2 pC/ms^2, 0-8400 KHz	4383-V	5	Titanium
Mounting, Bees wax	UA-0866	-	Bees Wax
0.14mm 10-32 UNF Cement stud	5	-	Brass
Super low-noise Cables	AO-0122-D	5	-
Two channel, Nexus Charge /conditioning amplifiers	2226654	3	-
24 bit, NI DAQ system	4431,4432	2	-
Non magnetic hammers	-	2	Wood, Plastic

4. Measurement procedures

The overall measurement procedure can be divided in to three parts.

- In the first part the MRI scanner was operating without a patient. The signal waveforms normally used for clinical diagnostics purpose were used to operate the MRI scanner and are tabulated in Table. 2, along with their duration, in the same order as used in the measurements. One accelerometer at each foot and one at the adjacent floor position were used to record the acceleration in a single measurement e.g. in measurement No.1 the floor accelerometer is placed near foot 1. The measurement procedure is repeated for foot and adjacent floor positions 2, 3 and 4 in subsequent measurements. The recorded data was divided into individual waveforms using Matlab with the aid of its plotting tools, for further analysis.

- In the second part the MRI scanner was not operating. A non-magnetic hammer was used to excite the MRI feet in the vertical direction and the acceleration were measured on each foot and floor position simultaneously. The procedure was repeated for each foot with several hammer strikes using two different hammers separately, one with a wooden hammer head and one made of hard plastic. For the analysis, five to seven less noisy hammer strikes are isolated from the measured time series and subsequently combined in a single vector. A suitable exponential window, e^{-at}, was used.

- In the third part the floor besides an MRI scanner foot was excited by the two hammers separately. The measurements and analysis procedure were similar to the second part.

Table 2. MRI waveforms used in measurements.

Sequence Name	Duration (seconds)
ASSET (callibration)	7
Ax T2 PROPELLER	105
T2 FSE	120
Ax FSPGR3D	258
Sag CUBF (CUBE flair)	250
DWI	54
SWAN	187

5. Results

Several measurements were performed in different sessions both with the MRI scanner in operation and when the MRI scanner was idle and the hammer excitation was used. Thus, a substantial number of analyses were carried out and a representative set of results from the experiments are presented below.

5.1 MRI waveforms and impulse strikes in time domain

During operation of the MRI scanner the acceleration at foot 1 and the floor position near foot 1, in the vertical direction, were measured (measurement No.1) and are shown in Fig. 2. Similarly Fig. 3a, presents the vertical acceleration measured on foot 4 (measurement No.4).

Impact excitation has been used to identify the transfer paths and to validate the transfer paths measured based on the MRI waveforms. Two different hammers were used. The results for both the hammers are identical and only one set is presented here. Five to seven hammer strikes were used in the measurements to enable adequate averaging for spectrum estimates. The acceleration produced

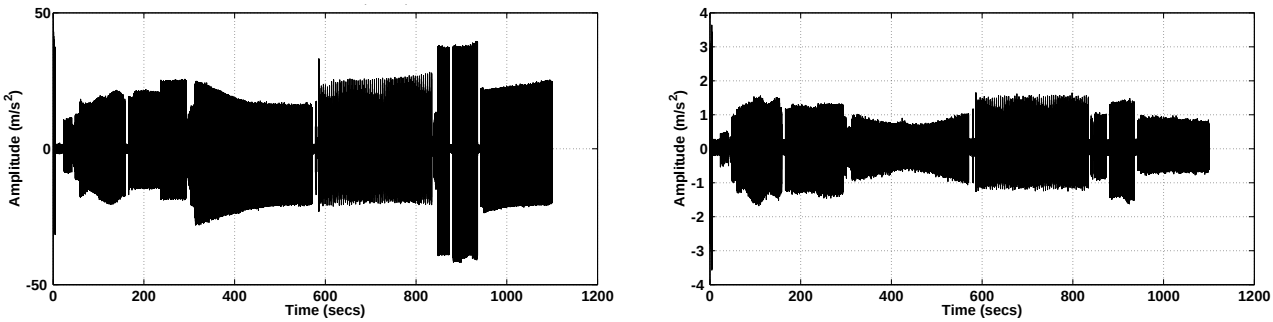

Figure 2. MRI waveforms in measurement No.1. (a). Acceleration record on foot 1. (b). Acceleration record on the floor adjacent to foot 1.

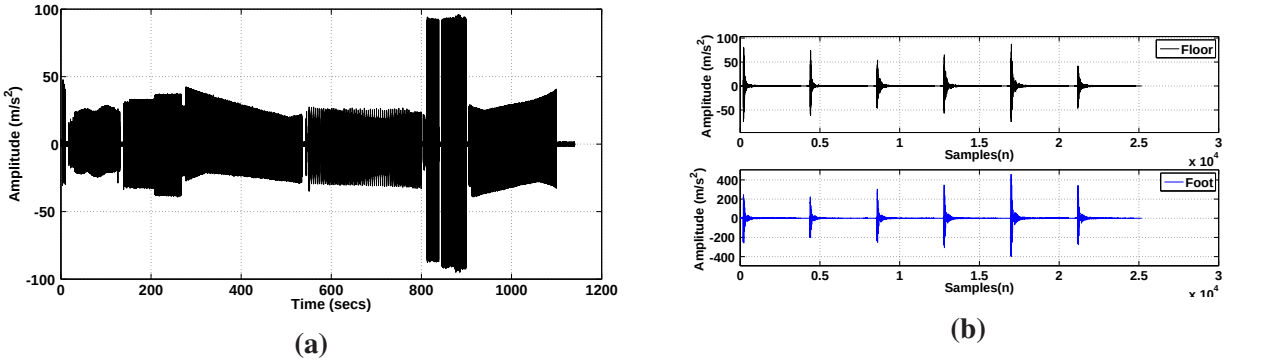

Figure 3. Acceleration record for MRI waveforms and hammer strikes. (a). Acceleration record on foot 4 in measurement No.4. (b). Acceleration measurement on foot 2 and adjacent floor position, using plastic hammer strikes on foot 2.

by the plastic hammer impacts on MRI scanner's foot 2 and the adjacent floor position are shown in Fig. 3b.

5.2 Coherence

The coherence plots between foot and floor measurements may reflect the noise in the measurements and show how much the signal on the floor/foot can be linearly explained from the signals on foot/floor. The coherence is measured for all the hammer strikes on foot, floor and for the MRI sequence measurements between a foot and floor. The coherence is relatively good between a foot and floor when the hammer impulse was made on the foot as compared to the strikes on the floor and for the MRI measurement waveforms. Estimates of the coherence between vertical acceleration at foot and floor for the wooden hammer impacts on foot 1 and for MRI sequence "SWAN" on foot 4 are shown shown in Fig. 4. An exponential window e^{-99t}, of length $2^{12} = 4096$, zero percent overlap and five to seven averages were used for the production of spectrum estimates.

5.3 Power spectrum (PS) and energy spectral density (ESD)

The MRI signal waveforms are periodic, thus, indicating that estimates of power spectra of the acceleration measured on the feet and floor positions are adequate. As a single MRI run consist of seven signal waveforms, tabulated in Table. 2. Therefore, the acceleration power spectra for each foot and adjacent floor positions are estimated for each signal sequence separately. A *Hanning* window of length $2^{12} = 4096$, with 50% overlap was used. The acceleration power spectra, for two different MRI waveforms, measured on foot 2 and adjacent floor position are shown in Fig. 5. From Fig. 5 a clear difference maybe observed between the floor and feet spectra, an indication of the amount of damping at different frequencies induced by the vibration isolators. When the MRI scanner was idle, hammer

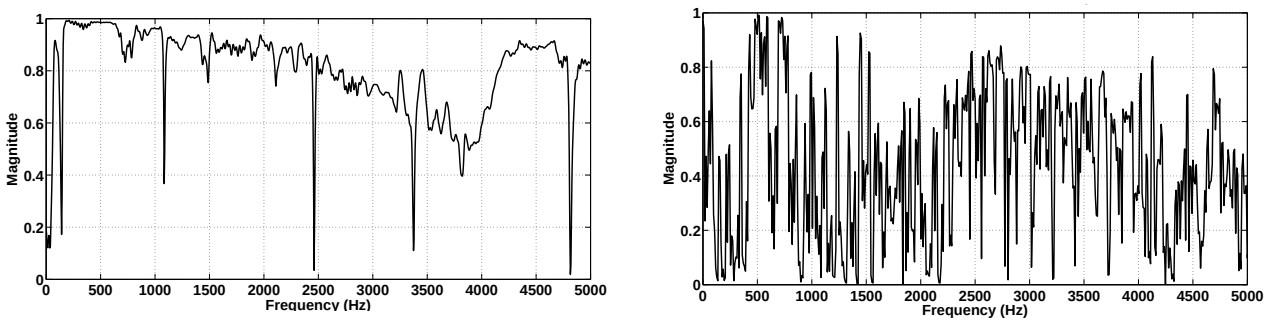

Figure 4. Coherence plots between vertical acceleration spectra at foot and floor. (a). Coherence plot between foot 1 and adjacent floor position using wooden hammer strike on foot 1. (b). Coherence plot(between foot 4 and nearby floor position for MRI sequence "SWAN"

impact excitation was used and the floor and feet acceleration were measured. The energy spectral density (ESD) was estimated for the floor and feet acceleration. In the ESD estimation procedure an exponential window e^{-99t} with length $2^{12} = 4096$ and no overlapping were used. The difference in the acceleration response for a certain foot and floor position depending on the type of hammer seemed to be negligible. However, a clear difference was observed depending on if the foot or the floor was excited by the hammer. From the ESD estimates plots shown in Fig. 6, for foot 1 and foot 3 along with their adjacent floor positions, a difference between the magnitude of the floor and the foot ESD can be observed, similar to the power spectra for the MRI waveforms.

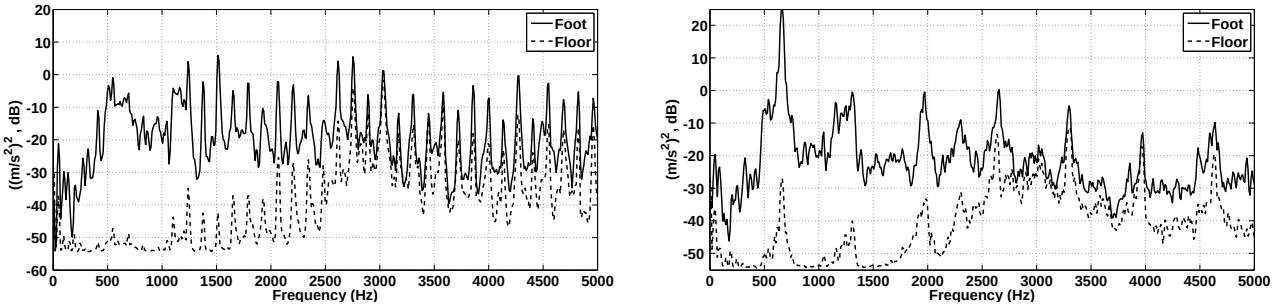

Figure 5. Acceleration power spectra measured on foot 2 and the adjacent floor position in measurement No.2 for two different MRI waveforms. (a). Acceleration power spectra of the MRI sequence "Ax T2PROPELLER". (b). Acceleration power spectra of the MRI sequence "DWI".

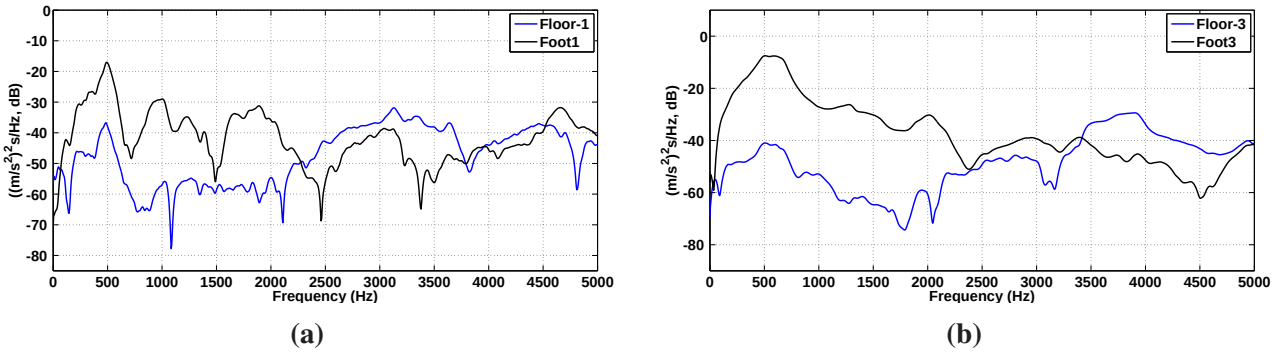

Figure 6. Energy spectral densities (ESD) of the acceleration on a foot and near by floor position. (a). ESD between foot 1 and adjacent floor position using wooden hammer with strike on the foot. (b). ESD between foot 3 and adjacent floor position using plastic hammer with strike on the foot.

5.4 Transmissibility functions

Ttransmissibilities $T_{ji}(f)$ were estimated between a foot and floor acceleration both for the case when the excitation is provided by operating the MRI scanner and for the case when the MRI scanner was idle and only hammer excitation. The analysis procedure i.e. the window function and selected overlap etc. is identical to the settings used for estimating the power spectra presented in section 5.3. The transmissibility for two different feet and adjacent floor positions for different MRI waveforms are presented in Fig. 7 and Fig. 8.

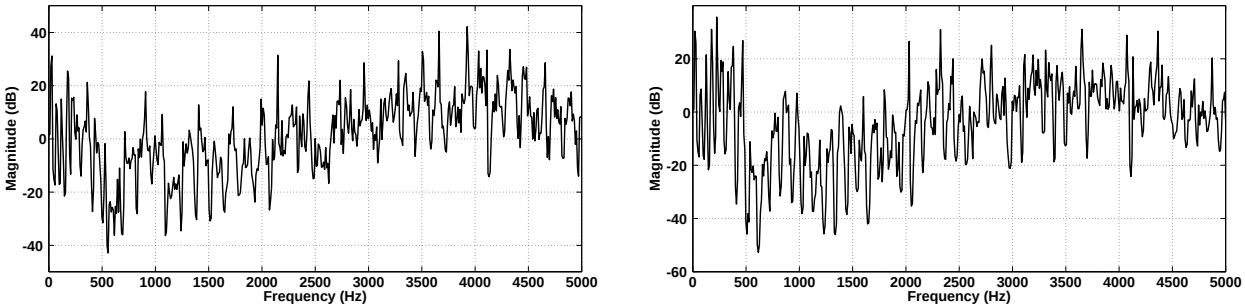

Figure 7. Transmissibility between foot 3 and adjacent floor position for two different MRI waveforms in measurement No.3. (a). Transmissibility for MRI sequence "Ax T2PROPELLERPSD". (b). Transmissibility for MRI sequence "Ax FSPGR3D".

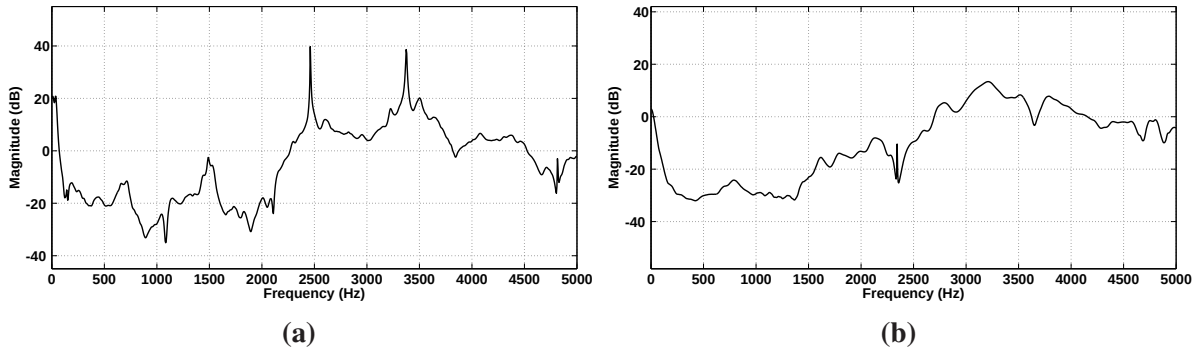

Figure 8. Transmissibility between acceleration spectra at two different feet and adjacent floor position, excitation provided by the two different hammer impulses. (a). Transmissibility between foot 1 and near by floor position, excited by the wooden hammer at the same foot. (b). Transmissibility between foot 2 and near by floor position, excited by the plastic hammer at the same foot.

6. Conclusions

From the results in Fig. 4 it follows that the coherence function estimates between foot and floor acceleration may indicate that the measurements are affected by uncorrelated noise. This noise may have several sources but the main source is likely to be the the cooling compressor, which runs continuously even when the MRI scanner is idle. The coherence for the hammer pulses also suggest measurements affected by uncorrelated noise, which is typical for impact excitation measurements. The coherence between a foot and adjacent floor acceleration is low for the hammer impulses on the floor as compared to those on the feet directly. The coherence between a foot and nearby floor acceleration using hammer excitation is generally higher as compared to the case of excitation by operating MRI.

From the time domain vibration signals shown in Fig. 2 and Fig. 3a, excited by the gradient coils in an operating MRI it seems like that the vertical acceleration differ between the feet. The

acceleration level of foot 1 is almost half as compared to the acceleration level of other three feet. The acceleration transferred to the floor also follows the same pattern.

The power spectra and ESD, Fig. 5 and Fig. 6, indicate an isolation between the feet and the floor of approx. 20 dB for frequencies below 2500 Hz and even an amplification may be observed for frequencies above 2500 Hz. A almost similar vibration isolation trend may be observed in the transmissibility plots, Fig. 7 and Fig. 8. The transmissibility plots, also suggest less isolation at frequencies below 500 Hz. The transmitted vibration may also produce structure borne noise in other parts of the building, which is off course heard.

7. Future work

Valuable information about the vibration transfer from the MRI scanner to floor is achieved through the analysis of transmissibility and the power spectra. To get a more understanding of the vibration transfer, further investigation is required. The vibration spectra will be compared to sound measurements in and outside the MRI scanner room to verify that if the sound outside MRI room is structural borne or not. Vibration measurements at other locations of the building will be made to verify the structure borne transmission. To get a more reliable system identification or vibration transfer characteristics the floor beneath the MRI will also be excited with random noise generated by a shaker.

REFERENCES

[1] Evans, J. B. Structural floor vibration and sound isolation design for a magnetic resonance imaging system, *Building Acoustics*, **12** (3), 207–23, (2005).

[2] Katsunuma, A., Takamori, H., Sakakura, Y. and Hamamura, Y. Quiet MRI with novel acoustic noise reduction, *Magnetic Resonance Materials in Physics, Biology and Medicine*, **13** (3), 139–144, (2002).

[3] Edelstein, W. A. et al. Making MRI Quieter, *Magnetic Resonance Imaging*, **20** (2), 155–163, (2002).

[4] Roozen, N. B., Koevoets, A. H. and den Hamer, A. J. Active Vibration Control of Gradient Coils to Reduce Acoustic Noise of MRI Systems, *IEEE/ASME Transactions on Mechatronics*, **13** (3), 325–334, (2008).

[5] Lin, T. R., O'Shea, P. and Mechefske, C. Reducing MRI gradient coil vibration with rib stiffeners, *Concepts in Magnetic Resonance Part B: Magnetic Resonance Engineering*, **35B** (4), 198–209, (2009).

[6] De Sitter, G., Devriendt, C., Guillaume, P. and Pruyt, E. Operational transfer path analysis, *Mechanical Systems and Signal Processing*, **24** (2), 416–431, (2010).

[7] De Klerk, D. and Ossipov, A. Operational transfer path analysis: Theory, guidelines and tire noise application, *Mechanical Systems and Signal Processing*, **24** (7), 1950–1962, (2010).

[8] Devriendt, C. and Guillaume, P. Identification of modal parameters from transmissibility measurements, *Journal of Sound and Vibration*, **314** (1-2), 343–356, (2008).

[9] Gajdatsy, P., Janssens, K., Desmet, W. and Van der Auweraer, H. Application of the transmissibility concept in transfer path analysis, *Mechanical Systems and Signal Processing*, **24** (7), 1963–1976, (2010).

[10] Devriendt, C., Steenackers, G., De Sitter, G. and Guillaume, P. From operating deflection shapes towards mode shapes using transmissibility measurements, *Mechanical Systems and Signal Processing*, **24** (3), 665–677, (2010).

[11] Kromulski, J. and Hojan, E. An application of two experimental modal analysis methods for the determination of operational deflection shapes, *Journal of Sound and Vibration*, **196** (4), 429–438, (1996).